Pergamon

PII: S0277-5387(96)00569-4

Polyhedron Vol. 16, No. 14, pp. 2465–2474, 1997

0277-5387/97 $17.00+0.00

Electronic and bonding properties of mixed-ligand copper(II) complexes of *N*-(2-pyridylethyl)picolinamide (PEPA). Molecular structures of [Cu(PEPA)(3-methylpyridine)(H_2O)](ClO_4), [Cu(PEPA)(4-methylpyridine)(H_2O)](ClO_4) and [Cu(PEPA)(4-methylimidazole)(H_2O)](H_2O)(ClO_4)

Chiou-Yuh Wu and Chan-Cheng Su*

Department of Chemistry, National Taiwan Normal University, Taipei 11718, Taiwan, Republic of China

(Received 7 October 1996; accepted 15 November 1996)

Abstract—Mixed-ligand *N*-(2-pyridylethyl)picolinamidocopper(II) complexes, Cu(pepa)(L)(H_2O)$_n$(ClO_4) [pepa = *N*-(2-pyridylethyl)picolinamide anion; L = imidazole (n = 0), *N*-methylimidazole (n = 1), 2-methylimidazole (n = 1), 4-methylimidazole (4MImH, n = 2), 3-methylpyridine (3Mpy, n = 1 and 2), and 4-methylpyridine (4Mpy, n = 1 and 2)], have been synthesized and characterized by elemental analyses, and electronic, vibrational and EPR spectroscopic measurements. Molecular structures of [Cu(pepa)(3Mpy)(H_2O)](ClO_4) (**1**), [Cu(pepa)(4Mpy)(H_2O)](ClO_4) (**2**) and [Cu(pepa)(4MImH)(H_2O)](H_2O)(ClO_4) (**3**) have been determined by X-ray diffraction methods. The structures of these complexes are square pyramidal with the pepa and a heterocyclic unidentate ligand forming the basal plane and an H_2O molecule on the apical position. The dihedral angles of the heterocyclic unidentate nucleus and the CuN_4 basal plane are 74.3° for **1**, 66.8° for **2** and 77.7° for **3**. The structures of other pepa complexes are suggested to be square pyramidal based on their spectroscopic data. The sequence of d orbitals was assigned as $d_{x^2-y^2} \gg d_{z^2} > d_{yz} > d_{xy} > d_{xz}$ for the square pyramidal complexes. The significant rise in energy of the d_{yz} orbital suggests that the central amido of the pepa ligand is a strong π-donor. Copyright © 1997 Elsevier Science Ltd

Keywords: N-(2-pyridylethyl)picolinamidocopper(II) complexes; X-ray structures; d-d spectra; EPR spectra; bonding; Gaussian analysis.

In the course of our studies on copper(II)–N bonding properties in mixed-ligand copper(II) complexes containing a tridentate and a heterocyclic unidentate ligand [1–4], we have found that the structures of these complexes and the orientations of the heterocyclic nuclei are varied depending on the bonding properties of the tridentate ligands. It is prominent that the glycylglycinato and the dipicolinato complexes comprise a heterocyclic unidentate ligand coplanar with the equatorial coordination plane. Further, their d orbitals consist of an unusual sequence of d_{yz} (d_{xz}) > d_{xy} > d_{xz}(d_{yz}), in contrast to the usual order that d_{xy} is higher in energy than both d_{xz} and d_{yz} in square planar, square pyramidal and elongated octahedral copper(II) complexes [5,6]. This infers that the central amido moiety of the glycylglycinato and the central pyridine of the dipicolinato are π-donors. Since we are interested in the bonding properties of the biologically important amido groups, we have studied a series of mixed-ligand *N*-(2-picolyl) picolinamidocopper(II) complexes [7] and revealed a

*Author to whom correspondence should be addressed.

similar $d_{yz} > d_{xy} > d_{xz}$ sequence and suggested accordingly the amido moiety of this tridentate ligand a π-donor. Herein we report the structures and spectroscopic properties of a series of mixed-ligand *N*-(2-pyridylethyl)picolinamidocopper(II) complexes and elucidate their electronic structures and bonding properties.

EXPERIMENTAL

Materials and preparations

Picolinic acid (Aldrich), 2-(aminoethyl)pyridine (Aldrich), *N*-methylimidazole (Aldrich), 2-methylimidazole (Merck), 4-methylimidazole (Merck), imidazole (Merck), 3-methylpyridine (TCI), 4-methylpyridine (TCI), $POCl_3$ (Merck), $Cu(ClO_4)_2 \cdot 6H_2O$ (Aldrich) and organic solvents were used as received.

N-(2-Pyridylethyl)picolinamide (pepaH) [8,9] was prepared as follows: To an anhydrous CH_2Cl_2 (100 cm^3) solution of picolinic acid (6.16 g, 0.05 mol), triethylamine (5.05 g, 0.05 mol), and 2-(aminoethyl)pyridine (6.11 g, 0.05 mol), phosphorus oxychloride (7.67g, 0.05 mol) in CH_2Cl_2 (40 cm^3) was added dropwise with constant stirring at 0°C. An additional amount of triethylamine (10.1 g, 0.1 mol) was added. After reaction at 0°C for 1.5 h and at room temperature for 1 h, the contents were neutralized with aqueous sodium bicarbonate. The organic layer was separated and evaporated to give a viscous residue. Yield, 6.9 g (61%). ^1H NMR (200 MHz, CD_3OD), δ/ppm: 3.17 (t, 2H), 3.92 (q, 2H), 7.19(t, 1H), 7.26(d, 1H), 7.41 (m, 1H), 7.67(m, 1H), 7.83(m, 1H), 8.19(m, 1H), 8.54(m, 1H), 8.60(d, 1H); ^{13}C NMR (400 MHz, CD_3OD), δ/ppm: 37.68, 39.05, 121.73, 122.30, 123.54, 126.18, 136.77, 137.39, 148.29, 149.48, 150.13, 159.33, 164.58. Mass *m/z* (relative intensity): M+1 = 228.2(20), M = 227.1 (19), 149.1(8), 135.1(54), 121.1(100), 93.1(65), 78(34).

The pepa complexes were prepared by the following general procedure: To a CH_3OH solution (10 cm^3) of $Cu(ClO_4)_2 \cdot 6H_2O$ (0.37 g, 1 mmol) and the unidentate ligand (2 mmol), *N*-(2-pyridylethyl)picolinamide (0.23 g, 1 mmol) in CH_3OH (5 cm^3) was added. After reaction for 2 h, the solution was stored for a few days to yield crystalline products, which were filtered and washed with ether and dried *in vacuo* over P_4O_{10}.

[*Cu*(*pepa*)(*ImH*)(ClO_4)]. Blue. Yield 69%. M.p. 175°C(dec.). IR (cm^{-1}): ν [N—H(ImH)] 3260m; ν (amido) 1616m, 1589s, 1570s; ν (ClO_4) 1095s, 1061s, 932m, 621s; ν [Cu—N(pepa)] 357m, 291m, 262m; ν [Cu—N(ImH)] 318m. Found: C, 41.3; H, 3.6; N, 15.1. Calc. for $C_{16}H_{16}N_5O_5ClCu$: C, 42.0; H, 3.5; N, 15.3%. Molar conductivity: 76 S cm^2 mol^{-1} in CH_3OH; 126 S cm^2 mol^{-1} in CH_3CN.

[*Cu*(*pepa*)(*ImH*)(H_2O)(BF_4)]. This blue complex was prepared as described above but by using $Cu(BF_4)_2 \cdot 6H_2O$. Yield 72%. M.p. 133°C(dec.). IR (cm^{-1}): ν (O—H) 3566ms; ν [N—H(ImH)] 3320s, br; ν (amido) 1622s, 1595s, 1568s; ν (BF_4) 1078vs; ν [Cu—N(pepa)] 351m, 303m, 262m; ν [Cu—N(ImH)] 318w. Found: C, 41.0; H, 3.9; N, 14.8. Calc. for $C_{16}H_{18}N_5O_2BF_4Cu$: C, 41.5; H, 3.9; N, 15.1%. Molar conductivity: 82 S cm^2 mol^{-1} in CH_3OH; 144 S cm^2 mol^{-1} in CH_3CN.

[*Cu*(*pepa*)(*NMIm*)(H_2O)(ClO_4)]. Blue. Yield 40%. M.p. 195°C(dec.). IR (cm^{-1}): ν (O—H) 3548m, 3322m; ν (amido) 1619s, 1593s, 1572s; ν (ClO_4) 1121vs, 1078vs, 621s; ν [Cu—N(pepa)] 351m, 283m, 254mw; ν [Cu—N(NMIm)] 313m. Found: C, 41.6; H, 3.8; N, 14.1. Calc. for $C_{17}H_{20}N_5O_6ClCu$: C, 41.7; H, 4.1; N, 14.3%. Molar conductivity: 81 S cm^2 mol^{-1} in CH_3OH; 123 S cm^2 mol^{-1} in CH_3CN.

[*Cu*(*pepa*)(*2MImH*)(H_2O)(ClO_4)]. Blue. Yield 69%. M.p. 206°C (dec.). IR (cm^{-1}): ν [O—H+N—H(2MImH)] 3273s,br; ν (amido) 1636s, 1598s, 1570s; ν (ClO_4) 1078s,br, 932m, 623s; ν [Cu—N(pepa)] 361m, 287m, 247m; ν [Cu—N (2MImH)] 320m. Found: C, 41.6; H, 3.5; N, 14.9. Calc. for $C_{17}H_{20}N_5O_6ClCu$: C, 41.7; H, 4.1; N, 14.3%. Molar conductivity: 85 S cm^2 mol^{-1} in CH_3OH; 124 S cm^2 mol^{-1} in CH_3CN.

[*Cu*(*pepa*)(*4MImH*)(H_2O)$_2$(ClO_4)]. Yield 77%. M.p. 115°C (dec.). IR (cm^{-1}): ν (O—H) 3570m, 3505m; ν (N—H) 3150ms,br; ν (amido) 1618s, 1593vs, 1570s; ν (ClO_4) 1094s,br, 933w, 625s; ν [Cu—N(pepa)] 355m, 286mw, 259m; ν [Cu—N(4MImH)] 311mw. Found: C, 39.5; H, 4.4; N, 13.5. Calc. for $C_{17}H_{22}N_5O_7ClCu$: C, 40.2; H, 4.4; N, 13.8%. Molar conductivity: 85 S cm^2 mol^{-1} in CH_3OH; 127 S cm^2 mol^{-1} in CH_3CN. The blue lamellar crystals suitable for X-ray structure determination were obtained by slow evaporation of a methanol solution.

[*Cu*(*pepa*)(*3Mpy*)(H_2O)$_2$(ClO_4)]. Yield 76%. M.p. 167°C (dec.). IR (cm^{-1}): ν (O—H) 3528m, 3316m, 3204m; ν (amido) 1620s, 1609s, 1595s, 1570s; ν (ClO_4) 1105s,br, 932w, 623s; δ (py) 413m; ν [Cu—N(pepa)] 353m, 284m, 251m; ν [Cu—N(py)] 309m. Found: C, 44.8; H, 4.2; N, 10.5. Calc. for $C_{19}H_{23}N_4O_7ClCu$: C, 44.0; H, 4.5; N, 10.8%. Molar conductivity: 82 S cm^2 mol^{-1} in CH_3OH; 124 S cm^2 mol^{-1} in CH_3CN. The blue columnar crystals [Cu(pepa)(3Mpy)(H_2O)(ClO_4)] suitable for X-ray structure determination were obtained by slow evaporation of a methanol solution.

[*Cu*(*pepa*)(*4Mpy*)(H_2O)$_2$(ClO_4)]. Yield. 75%. M.p. 163°C (dec.). IR (cm^{-1}): ν (O—H) 3522m, 3325m, 3204m; ν (amido) 1620s, 1609s, 1597s, 1570s; ν (ClO_4) 1098s,br, 932w, 623s; δ (py) 411mw; ν [Cu—N(pepa)] 353m, 291mw, 241m; ν [Cu—N(py)] 307mw. Found: C, 44.5; H, 4.1; N, 10.7. Calc. for $C_{19}H_{23}N_4O_7ClCu$: C, 44.0; H, 4.5; N, 10.8%. Molar conductivity: 90 S cm^2 mol^{-1} in CH_3OH; 123 S cm^2 mol^{-1} in CH_3CN. The blue tetragonal crystals [Cu(pepa)(4Mpy)(H_2O)(ClO_4)] suitable for X-ray structure determination were obtained by slow evaporation of a methanol solution.

Physical measurements

IR spectra were recorded as Nujol mulls or KBr pellets on a BIO-RAD FTS-40 FTIR spectrometer. A Hitachi U-3501 spectrophotometer was used for electronic spectra measurements. Solid samples were recorded as Nujol mulls on Whatman No. 1 filter paper. Deconvolution of the visible spectra into Gaussian component bands was performed on a VAX 6510 computer using the profile-fitting program CUVFIT [10]. EPR spectra were obtained by using a Bruker ER 200D spectrometer and calibrated with DPPH ($g = 2.0037$). Nuclear magnetic resonance (NMR) spectra were recorded with a Varian Gemini 2000 (200 MHz) and a JEOL EX 400 (400 MHz) spectrometer. Mass spectra were acquired on a Finnigan TSQ 700 spectrometer at an ionization potential of 70 eV. Siemens R3m/V and VAX 3300 computer-controlled Enraf–Nonius CAD 4 diffractometers were used for crystal data collection. Elemental analyses were carried out by the microanalysis laboratories of Taiwan University, Taipei.

Structure determination and refinement

Details of crystal data and processing parameters are summarized in Table 1. Twenty-five independent reflections with $15.08 \leqq 2\theta \leqq 30.22°$ for **1**, $15.78 \leqq 2\theta \leqq 28.48°$ for **2** and $12.26 \leqq 2\theta \leqq 28.44°$ for **3** were used for least-squares determination of the crystal systems and the cell constants. Diffractometer examination of the reciprocal lattice showed the space group to be $P2_1/n$ for **1** and $P2_1/c$ for **2** and **3**. Intensity data (ω–θ scan, $2\theta \leqq 55°$ for **1**; $2\theta \leqq 45°$ for **2**; $2\theta \leqq 50°$ for **3**) were collected at 298 K for two octants of the sphere ($0 \leqq h \leqq 9$, $0 \leqq k \leqq 16$, $-29 \leqq l \leqq 27$ for **1**; $0 \leqq h \leqq 7$, $0 \leqq k \leqq 26$, $-12 \leqq l \leqq 12$ for **2**; $0 \leqq h \leqq 6$, $0 \leqq k \leqq 14$, $-29 \leqq l \leqq 28$ for **3**) and corrected for Lorentz and polarization effects, but not for absorption. Three standard reflections were monitored every 50 reflections or every hour and showed no signs of crystal deterioration. The structures were solved by direct methods using Personal SDP software incorporated SIR for **1** and **3** and SHELXS for **2** [11–13] and refined by full-matrix least-squares on F values. Scattering factors and anomalous dispersion correction terms were taken from the *International Tables for X-ray Crystallography* [14]. The quantity minimized was $\Sigma w(|F_o| - |F_c|)^2$, with $w = 4F_o^2/\sigma^2(F_o^2)$. The hydrogen atoms included in the refinement were located in succeeding difference Fourier syntheses after the non-hydrogen atoms were refined anisotropically. All calculations were done on a 80486/33 PC. Additional material deposited at the Cambridge Crystallographic Data Centre comprises structure factors, atomic coordinates, anisotropic thermal parameters, and a full list of bond lengths and angles.

RESULTS AND DISCUSSION

Description of structures

The molecular structures of [Cu(pepa)(3Mpy)(H_2O)](ClO_4) (**1**), [Cu(pepa)(4Mpy)(H_2O)](ClO_4) (**2**) and [Cu(pepa)(4MImH)(H_2O)]$(H_2O)(ClO_4)$ (**3**) are shown in Figs 1, 2 and 3, respectively. Selected bond lengths and angles are listed in Table 2. The R values of complex **3** are large because of disorder and large thermal vibrations of the perchlorate anions. The cationic copper(II) complex moieties are normal. The structures of all three complexes are square pyramidal with the copper(II) ions bound by the tridentate anionic pepa and a unidentate ligand forming a basal plane and an H_2O on the z axis to complete a [4+1] elongated square pyramidal structure. The copper(II) ions are slightly above the CuN_4 plane in these com-

Table 1. Summary of crystal data and processing parameters for [Cu(pepa)(3Mpy)(H_2O)](ClO_4) (**1**), [Cu(pepa)(4Mpy)(H_2O)](ClO_4) (**2**) and [Cu(pepa)(4MImH)(H_2O)]$(H_2O)(ClO_4)$ (**3**)

	$C_{19}H_{21}N_4O_6ClCu$ (**1**)	$C_{19}H_{21}N_4O_6ClCu$ (**2**)	$C_{17}H_{22}N_5O_7ClCu$ (**3**)
F wt	500.39	500.39	507.39
Crystal size (mm)	$0.14 \times 0.18 \times 0.50$	$0.35 \times 0.41 \times 0.49$	$0.31 \times 0.50 \times 0.25$
Space group	$P2_1/n$	$P2_1/c$	$P2_1/c$
a (Å);	7.493(3)	7.322(1)	7.337(2)
b (Å); β (°)	12.591(2); 98.38(2)	24.426(2); 96.38(1)	12.294(1); 98.37(2)
c (Å);	22.403(5)	12.077(1)	22.393(3)
V (Å^3)	2090.4	2143.3	2176.8
Z	4	4	4
D_{calc} (g cm^{-3})	1.59	1.55	1.55
μ (mm^{-1})	1.21	1.18	1.31
Radiation (λ, Å)	Mo-K_α(0.71073)	Mo-K_α(0.71073)	Mo-K_α(0.71073)
Independent reflection	5009 [2884 $\geqslant$ 3.0 $\sigma(I)$]	2875 [2360 $\geqslant$ 3.0 $\sigma(I)$]	3170 [1228 $\geqslant$ 3.0 $\sigma(I)$]
Final R, R_w	0.046, 0.049	0.040, 0.043	0.070, 0.083
Largest shift Δ/σ	<0.01	<0.01	<0.01
Largest difference peak (e Å^{-3})	0.56	0.71	0.58

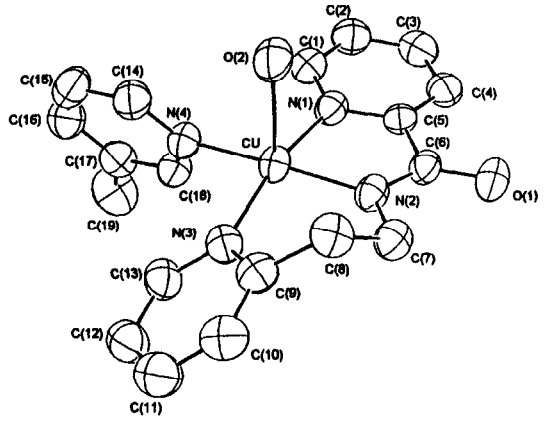

Fig. 1. Molecular structure of [Cu(pepa)(3Mpy)(H_2O)] (ClO_4) (**1**) with numbering scheme. Hydrogen atoms and perchlorate ion are omitted.

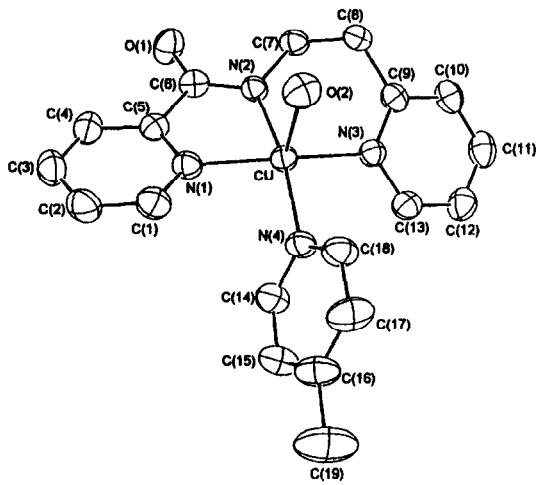

Fig. 2. Molecular structure of [Cu(pepa)(4Mpy)(H_2O)] (ClO_4) (**2**) with numbering scheme. Hydrogen atoms and perchlorate ion are omitted.

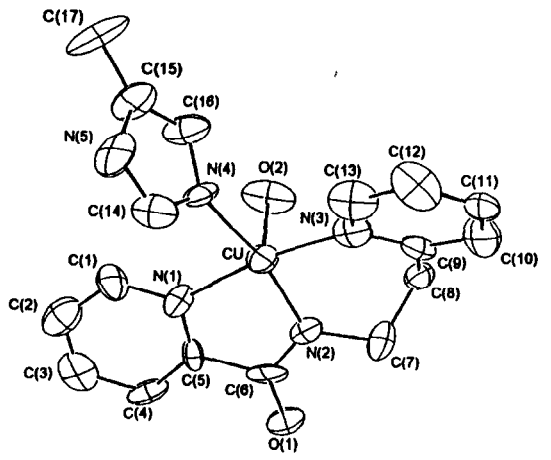

Fig. 3. Molecular structure of [Cu(pepa)(4MImH)(H_2O)] (H_2O)(ClO_4) (**3**) with numbering scheme. Hydrogen atoms, H_2O and perchlorate ion are omitted.

plexes. The deviations from the least-squares plane through the CuN_4 atoms are N(1) −0.0548, N(2) −0.0142, N(3) −0.0563, N(4) −0.0189 and Cu 0.1442 Å for **1**, N(1) −0.0219, N(2) −0.0470, N(3) −0.0269, N(4) −0.0477 and Cu 0.1435 Å for **2** and N(1) −0.0526, N(2) −0.0152, N(3) −0.0539, N(4) −0.0186 and Cu 0.1403 Å for **3**. In these three complexes, the N(1) pyridine nucleus and the amido moiety are coplanar and the N(3) pyridine rings are forced to tilt with a dihedral angle between the two terminal pyridine nuclei of 38.5° for **1**, 44.3° for **2** and 36.3° for **3**. The distances of the pepa coordination bonds, Cu—N(1) of 2.03 ± 0.01, Cu—N(2) of 1.94 ± 0.01 and Cu—N(3) of 2.045 ± 0.005 Å, are very much similar, as are their ∠N(1)—Cu—N(2) bite angles of 81.3 ± 0.2°. These facts suggest that the bonding modes of the pepa ligands in these three complexes are very similar.

It is noteworthy that the dimensions of the anionic amido portions, C(6)—O(1) of 1.24 ± 0.01 and C(6)—N(2) of 1.32 ± 0.02 Å, are comparable with those in the *N*-(2-picolyl)picolinamido (pmpa) complexes [7], C—O of 1.258 and C—N of 1.309 Å, and the glycylglycinato (glygly) complex [3], C—O of 1.257(7) and C—N of 1.310(7) Å. This suggests strongly that the π-delocalization in the N—C—O amide skeleton is analogous for the pepa, pmpa and glygly ligands and so their bonding abilities. Note, however, that although Cu—N(1) bond lengths are similar in pepa and pmpa complexes, the Cu—N(2) and Cu—N(3) distances are *ca* 0.03 Å longer for the pepa than for the corresponding pmpa complexes. Apparently, the puckered seven member ring in the pepa complexes makes the bonding somewhat weaker in these complexes.

The 3Mpy, 4Mpy and 4MImH unidentate ligands are bound nearly perpendicular to the basal plane, with the dihedral angles 74.3° for **1**, 66.8° for **2** and 77.7° for **3**. The Cu—N(4) coordination bonds are significantly longer than those of the corresponding pmpa complexes [7]. The bond lengths and angles of the pepa and the unidentate ligands are in the normal ranges. There are hydrogen bonds: O(2)···O(6), 2.893 and O(2)···O(1a), 2.782 Å in complex **1**; O(2)···O(6), 2.866 and O(2)···O(1a), 2.768 Å in complex **2**; and O(3)···N(5), 2.736, O(2)···O(4), 2.934 and O(2)···O(1a), 2.852 Å in complex **3**.

Spectroscopic studies

The IR spectral data for the pepa complexes are given in the Experimental section. There are usually two O—H stretching absorptions in 3500 cm^{-1} region assignable for the H_2O molecule bound directly to the central copper ion. The apical H_2O molecule of the water containing complexes may be identified by the appearance of OH stretching peaks in the 3500 cm^{-1} region. However, red shift to the 3300 cm^{-1} region was observed due to hydrogen bonds, resulting in

Table 2. Bond lengths (Å) and angles (°) for [Cu(pepa)(3Mpy)(H_2O)](ClO_4) (**1**), [Cu(pepa)(4Mpy)(H_2O)](ClO_4) (**2**) and [Cu(pepa)(4MImH)(H_2O)](H_2O)(ClO_4) (**3**)

[Cu(pepa)(3Mpy)(H_2O)](ClO_4) (**1**)			
Cu—N(1)	2.039(4)	Cu—N(2)	1.931(4)
Cu—N(3)	2.044(4)	Cu—N(4)	1.998(4)
Cu—O(2)	2.361(4)	O(1)—C(6)	1.254(6)
N(2)—C(6)	1.307(6)	N(2)—C(7)	1.458(6)
N(1)—Cu—N(2)	81.2(2)	N(1)—Cu—N(3)	167.6(2)
N(1)—Cu—N(4)	91.4(2)	N(2)—Cu—N(3)	92.7(2)
N(2)—Cu—N(4)	168.6(2)	N(3)—Cu—N(4)	92.9(2)
O(2)—Cu—N(1)	90.5(1)	O(2)—Cu—N(2)	93.7(1)
O(2)—Cu—N(3)	100.7(1)	O(2)—Cu—N(4)	95.1(2)
O(1)—C(6)—N(2)	127.1(4)	O(1)—C(6)—C(5)	119.2(4)
N(2)—C(6)—C(5)	113.6(4)	C(6)—N(2)—C(7)	117.2(4)
C(6)—N(2)—Cu	117.9(3)	Cu—N(2)—C(7)	124.7(3)
[Cu(pepa)(4Mpy)(H_2O)](ClO_4) (**2**)			
Cu—N(1)	2.042(4)	Cu—N(2)	1.937(3)
Cu—N(3)	2.050(3)	Cu—N(4)	2.001(4)
Cu—O(2)	2.405(3)	O(1)—C(6)	1.252(5)
N(2)—C(6)	1.318(6)	N(2)—C(7)	1.457(6)
N(1)—Cu—N(2)	81.3(1)	N(1)—Cu—N(3)	169.1(2)
N(1)—Cu—N(4)	91.3(1)	N(2)—Cu—N(3)	92.3(1)
N(2)—Cu—N(4)	167.1(2)	N(3)—Cu—N(4)	93.3(1)
O(2)—Cu—N(1)	90.2(1)	O(2)—Cu—N(2)	95.9(1)
O(2)—Cu—N(3)	99.3(1)	O(2)—Cu—N(4)	94.6(1)
O(1)—C(6)—N(2)	126.7(4)	O(1)—C(6)—C(5)	120.3(4)
N(2)—C(6)—C(5)	113.0(4)	C(6)—N(2)—C(7)	117.1(4)
C(6)—N(2)—Cu	117.3(3)	Cu—N(2)—C(7)	125.6(3)
[Cu(pepa)(4MImH)(H_2O)](H_2O)(ClO_4) (**3**)			
Cu—N(1)	2.02(1)	Cu—N(2)	1.95(1)
Cu—N(3)	2.05(1)	Cu—N(4)	2.01(1)
Cu—O(2)	2.38(1)	O(1)—C(6)	1.23(2)
N(2)—C(6)	1.34(2)	N(2)—C(7)	1.47(2)
N(1)—Cu—N(2)	81.5(5)	N(1)—Cu—N(3)	168.3(6)
N(1)—Cu—N(4)	90.2(5)	N(2)—Cu—N(3)	93.6(6)
N(2)—Cu—N(4)	168.2(6)	N(3)—Cu—N(4)	93.0(6)
O(2)—Cu—N(1)	88.2(5)	O(2)—Cu—N(2)	92.7(5)
O(2)—Cu—N(3)	102.7(5)	O(2)—Cu—N(4)	95.4(5)
O(1)—C(6)—N(2)	128(2)	O(1)—C(6)—C(5)	122(2)
N(2)—C(6)—C(5)	110(1)	C(6)—N(2)—C(7)	116(1)
C(6)—N(2)—Cu	119(1)	Cu—N(2)—C(7)	125(1)

mixing with the imidazole N—H stretching. The amide CO and CN stretching peaks observed in the 1600 cm^{-1} region are lowered by *ca* 30–40 cm^{-1} as compared with those of the free ligand. The Cu—N (pepa) stretches were tentatively assigned at *ca* 355, 290 and 260 cm^{-1} and the Cu—N stretches for the unidentate ligands were tentatively assigned at *ca* 315 cm^{-1}.

The visible and EPR spectroscopic data for the pepa copper(II) complexes are listed in Table 3. The complexes exhibit a single broad band in solid state mull spectra with λ_{max} in a narrow range of 577 to 590 nm except for [Cu(pepa)(2MImH)(H_2O)(ClO_4)] with λ_{max} at 564 nm. This is consistent with the X-ray structures of complexes **1**, **2** and **3** and suggests that the structures of these complexes are square pyramidal. The 2-methylimidazole complex is believed to be square pyramidal. The somewhat high ligand field strength of this complex is likely due to strong σ-donation of the 2-methylimidazole ligand (pK_a 7.77) [15]. Both ImH and NMIm complexes may have the perchlorate ion bind on the apical position to complete a square pyramidal structure. This is supported by the observed splitting of the broad perchlorate vibrational peaks in the 1100 cm^{-1} region. The λ_{max} values of the pepa complexes are higher in energy than the corresponding pmpa complexes, which appear in the region 581–606 nm [7]. This seems to disagree with

Table 3. Visible and EPR spectral data for pepa-Cu^{II} complexes

Compound[a]	LF bands[b] λ_{max} (ε), nm	EPR[c] g_z	g_y	g_x	A_z(Cu)	A_y(Cu)	A_y(N)	A_x(N)
$[Cu(pepa)(ImH)(H_2O)](BF_4)$	580/mull	(2.197	2.063)					
$[Cu(pepa)(ImH)](ClO_4)$	609(84)/CH_3OH	2.228	2.055	2.025	182	~13	~13	~13
	579/mull	[d]						
$[Cu(pepa)(NMIm)(H_2O)](ClO_4)$	604(86)/CH_3OH	2.231	2.055	2.024	179	~13	~13	~13
	590/mull	(2.211	2.065)					
$[Cu(pepa)(2MImH)(H_2O)](ClO_4)$	604(74)/CH_3OH	2.235	2.055	2.025	177	~13	~13	~13
	564/mull	[d]						
$[Cu(pepa)(4MImH)(H_2O)](H_2O)(ClO_4)$	599(154)/CH_3OH	2.216	2.051	2.015	176	~12	~12	~12
	580/mull	(2.213	2.067)					
$[Cu(pepa)(3Mpy)(H_2O)](H_2O)(ClO_4)$	604(89)/CH_3OH	2.229	2.055	2.024	179	~13	~13	~13
	581/mull	(2.220	2.067)					
$[Cu(pepa)(4Mpy)(H_2O)](H_2O)(ClO_4)$	628(119)/CH_3OH	2.227	2.055	2.024	187	~13	~13	~13
	577/mull	(2.204	2.059)					
	625(93)/CH_3OH	2.227	2.055	2.023	185	~13	~13	~13

[a] pepa = *N*-(2-pyridylethyl)picolinamido; ImH = imidazole; NMIm = *N*-methylimidazole; 2MImH = 2-methylimidazole; 4MImH = 4-methylimidazole; 3Mpy = 3-methylpyridine; 4Mpy = 4-methylpyridine.

[b] ε in $M^{-1}\,cm^{-1}$.

[c] X-band EPR spectra measured at 77 K in CH_3OH with hyperfine coupling constants in $10^{-4}\,cm^{-1}$. Powder data in parentheses.

[d] Exchange coupling.

the X-ray structural results that the pmpa ligands bind more strongly than the pepa ligands (*vide supra*). Analysis of the Gaussian component peaks may provide proper explanations (*vide infra*). In methanol solution, all of the complexes show λ_{max} in the 600 nm region indicating coordination of solvent molecules to the complexes.

The powder EPR spectra are of axial type of $g_{\parallel} > g_{\perp} > 2$, consistent with square pyramidal structures and indicative of $d_{x^2-y^2}$ ground state [16]. The glass spectra in methanol matrix exhibit the fine structures of rhombic spectral features. Quite analogous to the EPR spectra of pmpa complexes, there are six superhyperfine components with relative intensities close to the values of 1 : 2 : 3 : 3 : 2 : 1 for the A_y(Cu) and A_y(N) and followed by another set of five components of 1 : 2 : 3 : 2 : 1 for the A_x(N), as illustrated in Fig 4. Two component bands in each set are superimposed, resulting in a smaller difference of g_x and g_y (0.031) for these complexes than the pmpa complexes (0.038) [7]. It is proper to designate the y axis along the Cu—N(amido) in the CuN_4 plane and the x axis parallel to the direction of the two copper–pyridine (pepa) bonds. Apparently, the bonding strengths along the x and y directions are different. The energy levels of d_{yz} and d_{xz} are, therefore, non-degenerate, and their energy difference is expected to be smaller than that of the pmpa complexes. All of the g_z and A_z values are not much varied suggesting that these complexes comprise a very similar CuN_4 square plane analogous to those observed in complexes **1**, **2** and **3**.

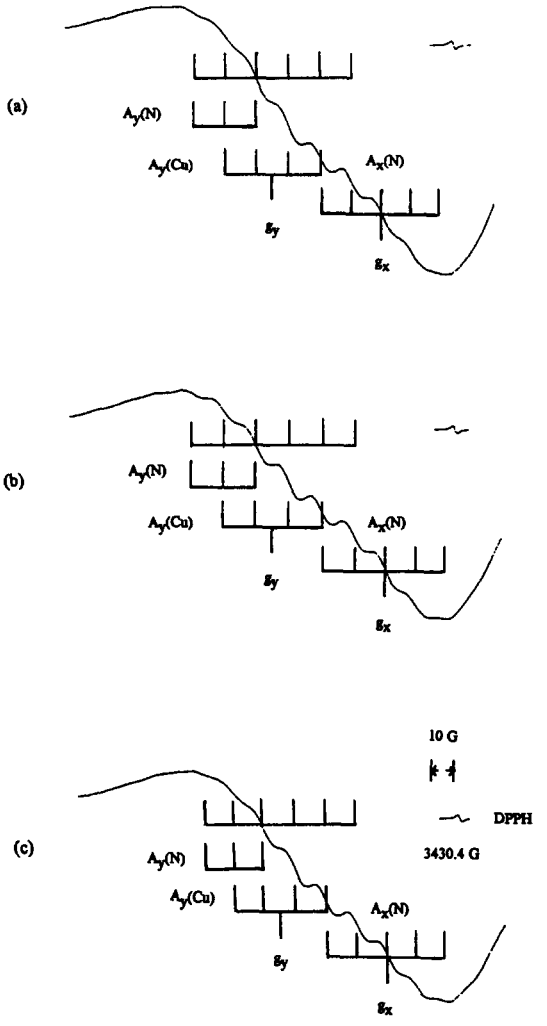

Fig. 4. The high-field region of X-band EPR spectra measured at 77 K in MeOH matrix for (a) [Cu(pepa)(3Mpy)(H_2O)](ClO_4)(H_2O); (b) [Cu(pepa)(4Mpy)(H_2O)](ClO_4)(H_2O); (c) [Cu(pepa)(4MImH)(H_2O)](ClO_4)(H_2O).

Electronic structures and bonding properties

The *d–d* spectra of the complexes were deconvoluted into Gaussian component bands. Starting from a set of four trial peaks, computer iteration processes for curve fitting were carried out until a minimum value of the reliability factor, R (see Table 4), was reached. Each of the complexes had an excellent fit with R less than *ca* 0.4% and showed a resulting set comprising four Gaussian peaks. This is in agreement with the rhombic EPR spectroscopic data that non-degeneracy for the d_{xz} and d_{yz} orbitals are suggested. Representative examples are shown in Fig. 5. The peak positions are presented in Table 4 along with their half-height widths and relative peak areas.

Similar to the structures of the pmpa complexes, namely, the complexes consist of a common tridentate and a nearly perpendicular heterocyclic unidentate ligand in the equatorial coordination plane, the following effects are anticipated: first, the $d_{x^2-y^2}$ level, being most involved in the copper-unidentate ligand bonding, will be considerably varied in energy due to the bonding capabilities of the unidentate ligands in the xy plane, resulting in shifts for all of the *d–d* transitions; secondly, defining the y axis along the Cu—N(2) bond, the d_{yz} level will not be affected by changing the unidentate ligand and the shift in the $d_{yz} \rightarrow d_{x^2-y^2}$ will mainly reflect the varying of the $d_{x^2-y^2}$ level; thirdly, the d_{xz} level will virtually not be affected, because the two coordinated groups of the terminal pyridine moieties are alike in the x direction. The shift in the $d_{xz} \rightarrow d_{x^2-y^2}$ transition will again reflect the variation of the $d_{x^2-y^2}$ level; finally, the d_{xy} level may be affected by changing the unidentate ligands and the shift in the $d_{xy} \rightarrow d_{x^2-y^2}$ transition will reflect the variation of the π-bonding capabilities of the unidentate ligands.

In this context, the energy difference between the d_{xz} and d_{yz} levels is expected to be nearly constant for these mixed-ligand pepa copper(II) complexes as was observed for the pmpa complexes [7]. Inspecting the Gaussian component peaks, the lowest energy peak having the smallest intensity can be assigned as

Table 4. Gaussian component bands for the visible spectra of pepa-Cu^{II} complexes

Band	ν(kK)	Area[a]	$\delta_{1/2}$[b]	Assignment
[Cu(pepa)(ImH)(H_2O)](BF_4)/ mull (0.20%)[c]				
I	13.9	0.98	3.03	d_{z^2}
II	15.7	2.73	3.05	d_{yz}
III	17.5	3.03	3.26	d_{xy}
IV	19.2	3.26	3.77	d_{xz}
[Cu(pepa)(ImH)](ClO_4)/ mull (0.25%)[c]				
I	14.0	0.50	2.39	d_{z^2}
II	15.7	2.33	2.67	d_{yz}
III	17.1	3.45	2.92	d_{xy}
IV	19.1	3.72	3.31	d_{xz}
[Cu(pepa)(NMIm)(H_2O)](ClO_4)/ mull (0.39%)[c]				
I	13.2	0.43	2.62	d_{z^2}
II	14.9	2.17	3.07	d_{yz}
III	16.5	3.63	3.10	d_{xy}
IV	18.4	3.77	3.32	d_{xz}
[Cu(pepa)(2MImH)(H_2O)](ClO_4)/ mull (R = 0.28%)[c]				
I	15.0	0.60	2.57	d_{z^2}
II	16.4	2.43	2.55	d_{yz}
III	17.9	3.10	2.67	d_{xy}
IV	19.8	3.87	3.55	d_{xz}
[Cu(pepa)(4MImH)(H_2O)](H_2O)(ClO_4)/ mull (R = 0.35%)[c]				
I	12.9	0.28	2.48	d_{z^2}
II	15.4	2.90	3.47	d_{yz}
III	17.1	3.41	3.43	d_{xy}
IV	18.8	3.41	3.74	d_{xz}
[Cu(pepa)(3Mpy)(H_2O)](H_2O)(ClO_4)/ mull (R = 0.36%)[c]				
I	13.1	0.61	2.64	d_{z^2}
II	15.3	2.96	3.30	d_{yz}
III	17.1	3.30	3.21	d_{xy}
IV	18.8	3.13	3.57	d_{xz}
[Cu(pepa)(4Mpy)(H_2O)](H_2O)(ClO_4)/ mull (R = 0.39%)[c]				
I	13.3	0.73	2.75	d_{z^2}
II	15.4	2.51	3.46	d_{yz}
III	17.0	2.95	3.43	d_{xy}
IV	18.8	3.81	3.89	d_{xz}

[a]Relative peak area in arbitrary scale based on a sum of 10.
[b]Half-width at $\varepsilon_{max}/2$.
[c]Reliability factor defined as $R = \Sigma|y_{obs,i} - y_{calc,i}|/\Sigma y_{obs,i}$.

$d_{z^2} \rightarrow d_{x^2-y^2}$ transition as reported in many square-pyramidal copper(II) complexes [16–19]. The energy difference between the highest and the lowest peaks of the rest three peaks is nearly constant (3.4 kK) for these complexes. The sequence of the d orbitals is therefore designed as $d_{x^2-y^2} \gg d_{z^2} > d_{yz} > d_{xy} > d_{xz}$. An average difference of 3.4 kK is reasonably in agreement with the corresponding values observed for the pmpa (3.5 kK) [7] and the glygly complexes (3.6 kK) [3].

Since the d_{yz} orbital is significantly higher in energy than the d_{xy} orbital, we conclude that the central amido moiety of the pepa ligand in these mixed-ligand copper(II) complexes is a strong π-donor. An average value of 3.4 kK of the energy difference between d_{yz} and d_{xz} orbitals in the pepa complexes is only marginally smaller than those for the pmpa and glygly complexes. However, this is in the right trend that the pepa ligand is not so tightly bound to the copper ion as the pmpa ligand. So, the d_{yz} orbital is not raised as much as in the pmpa complexes. The $d_{yz} \rightarrow d_{x^2-y^2}$ transition energy is, therefore, higher for the pepa complexes than the pmpa ones. In turn, the λ_{max} values show in the higher energy region for the pepa com-

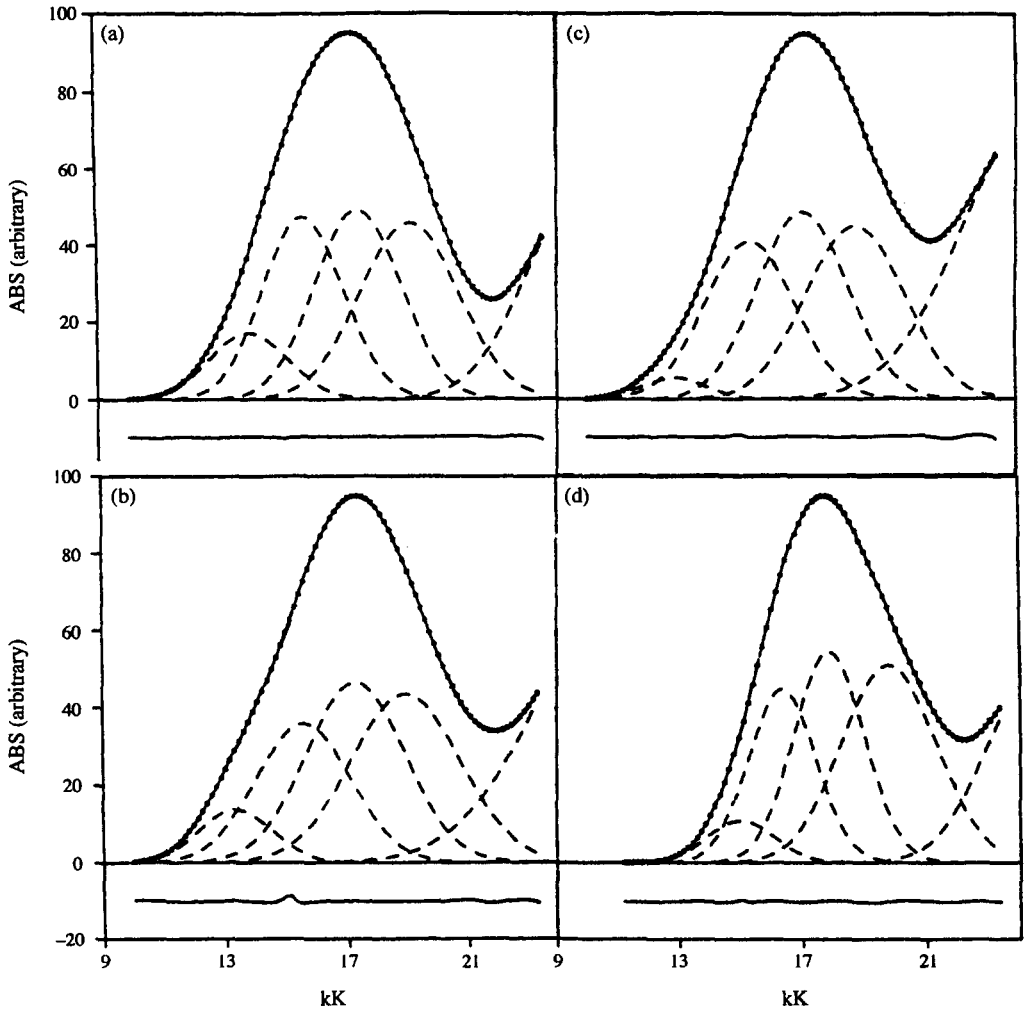

Fig. 5. Visible spectra and Gaussian line-shape analysis with difference plots of (a) [Cu(pepa)(ImH)(H_2O)](BF_4), R = 0.20%; (b) [Cu(pepa)(4Mpy)(H_2O)](ClO_4)(H_2O), R = 0.39%; (c) [Cu(pepa)(4MImH)(H_2O)](ClO_4)(H_2O), R = 0.35%; (d) [Cu(pepa)(2MImH)(H_2O)](ClO_4), R = 0.28%. (—), observed spectrum; (···), Gaussian components; (*) profile-fitting points.

plexes because the *d–d* band maximum appears in the overlapping range of the $d_{yz} \rightarrow d_{x^2-y^2}$ and $d_{xy} \rightarrow d_{x^2-y^2}$ component peaks.

Acknowledgements—Financial support from the National Science Council of the Republic of China (NSC85-2113-M-003-001) is gratefully acknowledged. We thank Professor C.-H. Ueng for assistance with X-ray work.

REFERENCES

1. Su, C.-C. and Wu, C.-Y., *J. Coord. Chem.* 1994, **33**, 1.
2. Su, C.-C. and Li, C.-B., *Polyhedron* 1994, **13**, 825.
3. Chiu, H.-J., Su, C.-C., Wang, S.-L. and Liao, F.-L., *Trans. Met. Chem.* 1994, **19**, 413.
4. Su, C.-C. and Chiu, S.-Y., *Polyhedron* 1996, **15**, 2623.
5. Hathaway, B. J., in *Comprehensive Coordination Chemistry* ed. G. Wilkinson, R. D. Gillard and J. A. McCleverty, Vol. 5. Pergamon Press, Oxford, 1987, pp. 594–774.
6. Burton, V. J. and Deeth, R. J., *J. Chem. Soc., Chem. Commun.* 1995, 573.
7. Wu, C.-Y. and Su, C.-C., *Polyhedron*, 1997, **16**, 383.
8. For abbreviation, see Table 3.
9. Vig, O. P., Trehan, I. R., Kad, G. L. and Ghose, J., *Indian. J. Chem.* 1992, **21B**, 748.
10. Wang, S. L., Wang, P. C. and Nieh, Y. P., *J. Appl. Cryst.* 1990, **23**, 520.
11. Frenz, B., *Personal SDP Reference Manual.* B. A. Frenz & Associates Inc., Houston, TX, U.S.A., 1992.
12. Sheldrick, G. M., *SHELXS*86. *Program for the Solution of Crystal Structures.* University of Gottingen, Germany, 1985.
13. Burla, M. C., Camalli, M., Cascarano, G., Giacovazzo, C., Polidori, G., Spangna, R. and Viterbo, D., *J. Appl. Cryst.* 1989, **22**, 389.

14. *International Tables for X-ray Crystallography*, Vol 4. Kynoch Press, Birmingham, 1974.
15. Liang, F., McCracken, J. and Peisach, J., *J. Am. Chem. Soc.* 1990, **112,** 9035.
16. Hathaway, B. J. and Tomlison, A. A. G., *Coord. Chem. Rev.* 1970, **5,** 1.
17. Hathaway, B. J. and Billing, D. E., *Coord. Chem. Rev.* 1970, **5,** 143.
18. Tomlison, A. A. G. and Hathaway, B. J., *J. Chem. Soc.* (*A*) 1968, 1685.
19. Su, C.-C., Lin, J.-S., Lin, Y.-L., Wang, S.-L. and Liao, F.-L., *J. Coord. Chem.* 1993, **30,** 91.